Journal of Power Sources 196 (2011) 827–834

Contents lists available at ScienceDirect

Journal of Power Sources

journal homepage: www.elsevier.com/locate/jpowsour

A micro-fabricated hydrogen storage module with sub-atmospheric activation and durability in air exposure

Xi Shan[a,*], Joe H. Payer[a], Jesse S. Wainright[b], Laurie Dudik[b]

[a] Corrosion and Reliability Engineering, Department of Chemical and Biomolecular Engineering, University of Akron, 302 Buchtel Common, Akron, OH 44325, USA
[b] Department of Chemical Engineering, Case Western Reserve University, Cleveland, OH 44106, USA

ARTICLE INFO

Article history:
Received 11 June 2010
Accepted 21 July 2010
Available online 1 August 2010

Keywords:
$CaNi_5$
Fuel cell
Hydrogen storage
$LaNi_{4.7}Al_{0.3}$
Thin-film

ABSTRACT

The objective of this work was to develop a hydrogen storage module for onboard electrical power sources suitable for use in micro-power systems and micro-electro-mechanical systems (MEMS). Hydrogen storage materials were developed as thin-film inks to be compatible with an integrated manufacturing process. Important design aspects were (a) ready activation at sub-atmospheric hydrogen pressure and room temperature and (b) durability, i.e. capable of hundreds of absorption/desorption cycles and resistance to deactivation on exposure to air. Inks with palladium-treated intermetallic hydrogen storage alloys were developed and are shown here to be compatible with a thin-film micro-fabrication process. These hydrogen storage modules absorb hydrogen readily at atmospheric pressure, and the absorption/desorption rates remained fast even after the ink was exposed to air for 47 weeks.

1. Introduction

The objective of this work was to develop a hydrogen storage module for onboard electrical power sources and suitable for use in micro-power systems and micro-electro-mechanical systems (MEMS). At Case Western Reserve University, researchers are now developing a number of micro-power systems, including a micro-fabricated hydrogen–air PEM fuel cell system with integrated fuel storage for autonomous operation [1]. Another development is a new type of low-pressure nickel–hydrogen battery which uses hydrogen gas directly from hydrogen storage materials [2,3]. Both of these and other micro-power systems need an effective and durable hydrogen fuel source that operates under ambient condition.

For micro-power systems, a critical factor related to the energy capacity is the voluminal capacity of the hydrogen storage method. Due to safety and mechanical strength limitations, the working pressure and temperature of the hydrogen storage module should be near ambient condition. In the micro-power systems, the hydrogen source is integrated with the micro-power systems, so it should be compatible with the working environments, such as the durability on exposure to high humidity in the fuel cell environment. Also, the hydrogen storage capacity and absorption/desorption kinetics should not be significantly affected by the micro-fabrication process, which involves mixing the hydrogen storage alloy powder with polymer binders and baking in air to form thin-film ink. For longer service life and lower cost, the hydrogen source should be reusable. In order to provide high current, the hydrogen release rate should be fast.

A basic property of the metal hydride is the pressure-composition-isotherm (PCI). The PCI is the relationship between the hydrogen pressure and hydrogen composition in the hydride under constant temperature. Usually, the hydrogen composition is expressed as the ratio between the number of hydrogen atoms stored in the metal to the number of metal atoms H/M. On the PCI curve, there is usually a hysteresis between the absorption process and desorption process, and the desorption pressure is lower than the absorption pressure for the same hydrogen composition. Each process shows a plateau region, in which the hydrogen composition changes over a wide range while the hydrogen pressure only changes slightly. The middle part of the plateau is defined as the plateau pressure. The working pressure of the metal hydride is near the plateau pressure.

Palladium is the first metal that was found to store hydrogen. For palladium to absorb hydrogen, no activation is needed [4]. In our work, palladium was used in the proto-type of the micro-fabricated PEM fuel cell. However due to the low desorption pressure at room temperature, which is 0.83 kPa [5], hydrogen in palladium could not be released effectively at room temperature. Hydrogen storage alloys with applicable working pressures and high storage capacities were identified. However, a common characteristic of the hydrogen storage alloys is that they need a form of activation before they can absorb hydrogen to maximum capacity and reach the maximum hydriding/de-hydriding rate. The activation involves

* Corresponding author. Tel.: +1 330 972 2968; fax: +1 330 972 5141.
E-mail address: shan@uakron.edu (X. Shan).

0378-7753/$ – see front matter © 2010 Elsevier B.V. All rights reserved.
doi:10.1016/j.jpowsour.2010.07.069

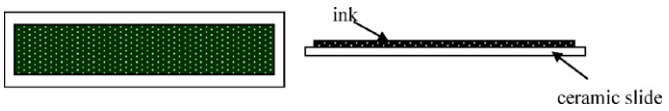

Fig. 1. Scheme of thin-film ink.

exposing the hydrogen storage alloy to high pressure and/or high temperature, which are far beyond the mechanical limit for the micro-power systems of interest. Also, when the activated materials are exposed to air, they soon lose the capability to absorb hydrogen and need to be activated again. In order to use hydrogen storage metals and alloys in the micro-power systems, a treatment was needed to lower the activation pressure and temperature and to keep the activity of the alloys.

By modifying the surface composition/structure of the hydrogen storage alloys, the activation performance and absorption/desorption kinetics of hydrogen storage materials can be improved. The surface modification can be chemical treatment [6,7], coating with Pt group metals by electroless plating [8], or mechanical grinding the intermetallic alloys with catalysts to nano-size particles [9–11].

It was found that, mechanically grinding a small amount of palladium or platinum with the hydrogen storage alloys was shown to greatly increase the hydrogen storage performance and lower the activation pressure to sub-atmosphere [12,13]. The resistance to air exposure was also greatly increased [14]. The mechanism of the increased performance and durability has been presented [13]. In this work, the performances of the palladium-treated alloys and thin-film inks made with the palladium-treated alloys were developed and evaluated.

2. Materials and methods

2.1. Materials

The palladium used in this study had a surface area of 20 $m^2\ g^{-1}$ and was from Alfa Aesar Inc. The intermetallic alloys investigated were $LaNi_{4.7}Al_{0.3}$ and $CaNi_5$, and were obtained from Ergenics Inc., Ringwood, NJ. To prepare the palladium-treated alloy, the as-received alloy particles were mixed with palladium powder in the weight ratio of 10:1 and ground with mortar and pestle in air for 25 to 30 min. Procedure on the preparation of the palladium-treated hydrogen storage alloys was reported elsewhere [12,14].

The application of the hydrogen storage intermetallic alloys in the micro-power system was in the form of thin-film ink composed of a mixture of the palladium-treated alloy and polymer binders. To prepare the ink, the solvent and the polymer binder were mixed together first and a homogenizer was used to make a uniform solution. Hydrogen storage alloy was added to the solution and mixed together with the solution into a uniform paste. The paste was applied on an alumina ceramic slide as a thin-film as shown in Fig. 1. The size of the ceramic slide was 50 mm by 12.5 mm. The ink was dried in air or oven to remove the solvent from the paste. After drying, the thickness of the ink was about 0.2–0.5 mm. Two polymer binders were studied, and they are polyethylene oxide (PEO) and polyvinylidene fluoride (PVDF). For the ink made with PEO, it contained 0.5 wt.% binder, while for the ink made with PVDF, the amount of binder was 2 wt.%.

The composition of the hydrogen gas was: H_2 99.95%, O_2 10 ppm, N_2 400 ppm, H_2O 32 ppm.

2.2. Methods

The hydrogen absorption/desorption and the pressure-composition isotherm (PCI) tests were carried on a Sievert's apparatus at room temperature. Hydrogen absorption/desorption cycle tests were performed with a modified Sievert's apparatus, which had four sample containers and each sample container could be controlled independently. The cyclic test apparatus was made with VCR® fittings and bellows valves from Swagelok Company. The sample container for the cyclic test and the Sievert's apparatus were interchangeable. Fig. 2 shows the test instrument for the cyclic test. The data collection and system control were performed with LabVIEW®. The cycle tests were carried out at room temperature, and the four samples were tested together. The absorption/desorption schedule was 10 min absorption under approximately 110 kPa hydrogen followed by 10 min desorption in vacuum, and the cycle was repeated for as many as 5000 cycles. During the absorption process, the pressure change was less than 5% of the initial applied pressure, so essentially the tests were run under constant pressure. In order to examine performance of the sample, the absorption/desorption properties of each sample were measured individually after every 250 cycles. After every 1000 cycles, the sample container was transferred from the cycle test station to the Sievert's apparatus with the sample in vacuum for the measurement of the PCI behavior, and then the samples were taken out from the sample containers for structural integrity examination. The total air exposure time during structural integrity examination was between 24 and 72 h.

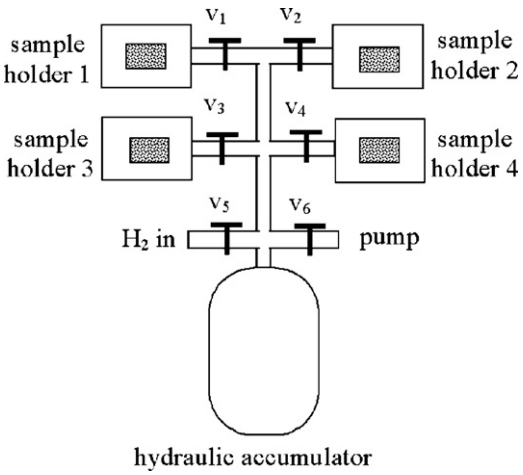

Fig. 2. Absorption/desorption cycle test instrument.

For the cycle test, the effect of humidification was examined. Hydrogen was used in the as-received condition was tested, and hydrogen with 75% relative humidity was also tested. To obtain 75% relative humidity, the hydrogen gas flowed slowly through a 500 ml gas wash bottle which contained 200 ml saturated NaCl solution before entering the cycle test instrument [15].

The effects of cyclic exposure on the structural integrity of ink modules and intermetallic particles were examined by scanning electron microscopy (SEM) and X-ray diffraction (XRD). The SEM analysis was performed on Philips XL-30, XRD analysis was performed on a computer controlled Scintag XRD with DMSNT software.

3. Results

The hydrogen storage performance of $LaNi_{4.7}Al_{0.3}$ and $CaNi_5$ were improved by Pd-treatment composed of grinding with small amount of palladium [12,14]. Freshly ground, un-treated $CaNi_5$ could not be activated under atmospheric hydrogen pressure in short time at room temperature. Freshly ground, un-treated $LaNi_{4.7}Al_{0.3}$ could be activated under atmospheric pressure hydrogen at room temperature, but it lost the atmosphere pressure

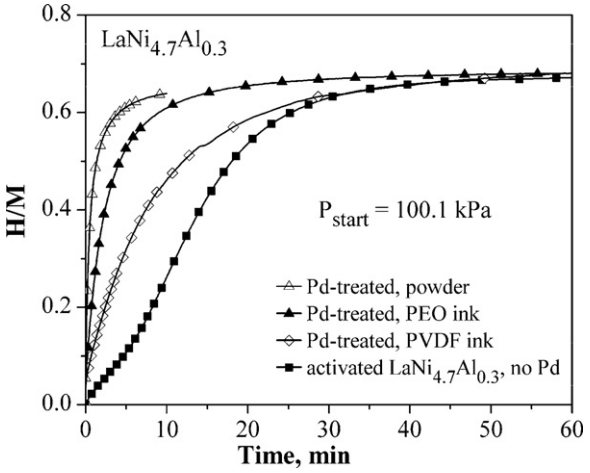

Fig. 3. First hydrogen absorption (charging) of thin-film inks with Pd-treated $LaNi_{4.7}Al_{0.3}$.

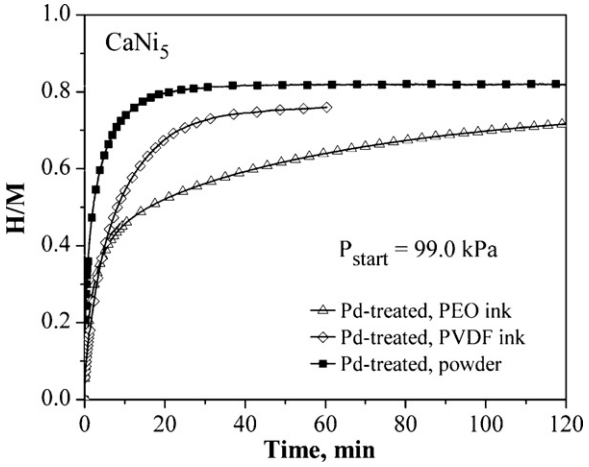

Fig. 4. First hydrogen absorption (charging) of thin-film inks with Pd-treated $CaNi_5$.

activation behavior in less than 100 h after being exposed to air [14]. After grinding with palladium, these two alloys could absorb hydrogen readily below atmospheric pressure even after being exposed to air for more than 2 years, and both the hydrogen absorption and desorption rates were increased significantly compared to the samples without the palladium-treatment [12,14].

After the micro-fabrication process and air exposure, the inks were still active under atmospheric pressure at room temperature, and kept the fast absorption/desorption rates. The storage capacities were not significantly affected by the micro-fabrication process. Fig. 3 shows the first hydrogen absorption of the palladium-treated $LaNi_{4.7}Al_{0.3}$ PEO and PVDF thin-film inks under 100.1 kPa hydrogen. For comparison, the first hydrogen absorption of the freshly prepared palladium-treated $LaNi_{4.7}Al_{0.3}$ powder sample and the absorption of the activated (after 5 absorption/desorption cycles under atmosphere hydrogen) freshly ground $LaNi_{4.7}Al_{0.3}$ sample without palladium-treatment are also shown in Fig. 3. As their corresponding palladium-treated alloys, the inks could easily absorb hydrogen in the first absorption under atmosphere hydrogen. While the inks had faster absorption rates than un-treated powders, the absorption rates of the inks were slower than those of the corresponding palladium-treated powder samples in the first absorption. The absorption half reaction times for palladium-treated $LaNi_{4.7}Al_{0.3}$ PEO ink was 1.8 and 9.8 min for palladium-treated $LaNi_{4.7}Al_{0.3}$ PVDF ink. Those compare to 0.4 min for the palladium-treated $LaNi_{4.7}Al_{0.3}$ before the micro-fabrication process and 12 min for the un-treated freshly ground $LaNi_{4.7}Al_{0.3}$. Compared to powders, while the Pd-treatment was effective for inks, the micro-fabrication process decreased the absorption rate of palladium-treated $LaNi_{4.7}Al_{0.3}$.

Fig. 4 shows the first hydrogen absorption of the freshly prepared palladium-treated $CaNi_5$ PEO and PVDF thin-film inks under 99.0 kPa hydrogen. For $CaNi_5$ inks in the first hydrogen absorption, the absorption half reaction times were 5.3 min for the ink with PEO binder and 4.6 min for the ink with PVDF binder, and those compare to 1.7 min for the powder sample. The micro-fabrication process slightly decreased the absorption rate of palladium-treated $CaNi_5$ powder, and it also showed similar effect on the desorption process of palladium-treated $CaNi_5$.

Inks made from both palladium-treated $LaNi_{4.7}Al_{0.3}$ and $CaNi_5$ alloys kept the atmosphere activation property after extended air exposure. The longest air exposure tested was 47 weeks on palladium-treated $LaNi_{4.7}Al_{0.3}$ PEO ink. After this extended long-time air exposure, the ink could still absorb hydrogen readily in the first hydrogen absorption under atmosphere hydrogen. While the polymer binders and/or the ink preparation process caused some degradation to the absorption rates of the palladium-treated powders, the inks made with the palladium-treated alloys still kept the atmosphere activation property. Furthermore, the hydrogen absorption rates of these inks were significantly better than the alloys without palladium-treatment.

To examine durability, absorption/desorption cycle tests were carried on fabricated storage modules to study the absorption/desorption properties as well as the structural integrity of the ink modules. The effect of cycle tests on the absorption rates of palladium-treated alloy inks was small in the un-humidified hydrogen. Fig. 5 shows the absorption behavior of the PEO ink prepared with palladium-treated $LaNi_{4.7}Al_{0.3}$ as a function of cycle number in the un-humidified hydrogen. During the first 2000 cycles, the absorption rate increased with increasing the cycle number, and then the absorption rate became nearly constant with increasing the cycle number up to 5000 cycles. The half reaction time for the first hydrogen absorption was 1.8 min, and after 5000 cycles the absorption half reaction time was 1.1 min. Fig. 6 shows the effect of cycle number on the absorption of palladium-treated $CaNi_5$ PEO ink. The absorption rate decreased slightly in the first 1000 cycles, and then it increased with increasing cycle number until 2500 cycles. After 2500 cycles the absorption rate was essentially constant.

The effects of cycle test on the hydrogen storage capacities of the thin-film inks varied with the alloy used. Inks made with

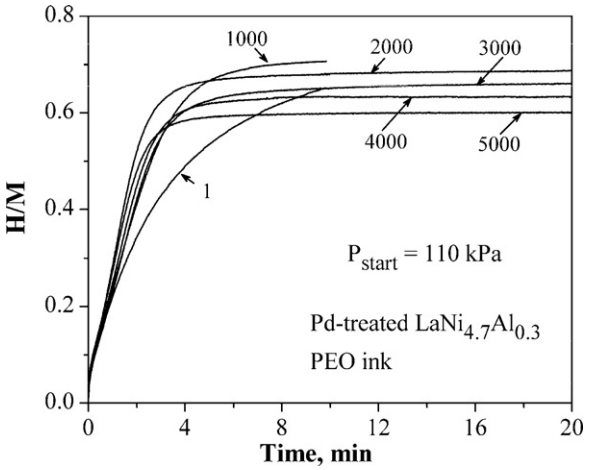

Fig. 5. Effect of absorption/desorption cycles on the absorption of Pd-treated $LaN_{4.7}Al_{0.3}$, PEO ink.

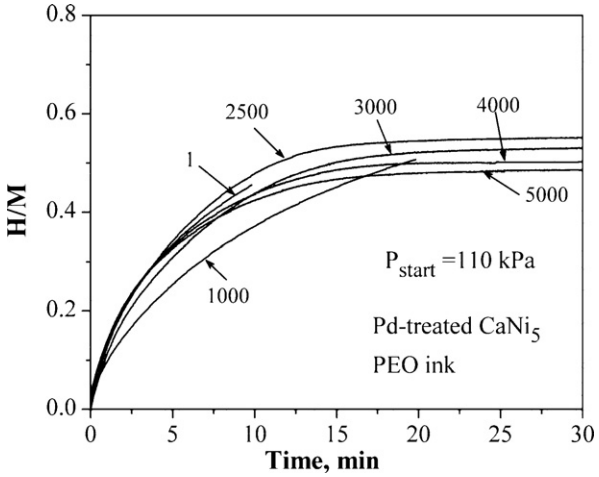

Fig. 6. Effect of absorption/desorption cycles on the absorption of Pd-treated $CaNi_5$ PEO ink.

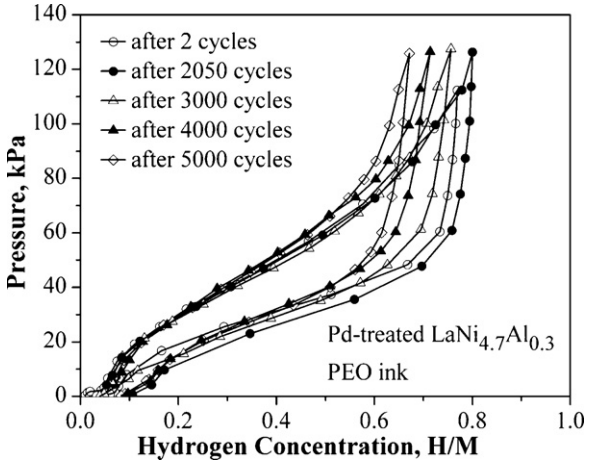

Fig. 8. Effect of absorption/desorption cycles on PCI of Pd-treated $LaNi_{4.7}Al_{0.3}$, PEO ink in un-humidified hydrogen.

$LaNi_{4.7}Al_{0.3}$ were more stable than the inks made with $CaNi_5$. The equilibrium H/M of the palladium-treated $LaNi_{4.7}Al_{0.3}$ PEO ink as a function of cycle number is shown in Fig. 7. The equilibrium H/M decreased from 0.71 to 0.60 after 5000 cycles, i.e. a decrease of 14%. During each 1000 cycles, the equilibrium hydrogen concentration kept almost constant, and the air exposures after each 1000 cycles caused a hydrogen equilibrium concentration decrease for the following 1000 cycles. The cyclic stability of the palladium-treated $LaNi_{4.7}Al_{0.3}$ powder sample was also tested, and the storage capacity changes with absorption/desorption cycle showed the same tendency as the ink sample as shown in Fig. 7. For the palladium-treated $CaNi_5$ PEO ink sample, the absorption equilibrium hydrogen concentration was 0.5 H/M after 5000 cycles. The freshly prepared palladium-treated $CaNi_5$ PEO ink absorbed 0.77 H/M hydrogen, so the decrease of the equilibrium concentration was 0.27 H/M or 35% of the original capacity. The decrease of $CaNi_5$ PEO ink capacity was about twice that of the $LaNi_{4.7}Al_{0.3}$ PEO ink.

The capacity decrease of the alloys in the cycle test was indicated by decrease of the width of the plateau region of the alloy. The plateau slope and the plateau pressures of the alloy were basically not affected by the cycle test. Figs. 8 and 9 show the effects of hydrogen absorption/desorption cycle test on the PCI behavior of palladium-treated $LaNi_{4.7}Al_{0.3}$ and $CaNi_5$ PEO inks, respectively. For both samples, the maximum H/M in the tested pressure range decreased with increasing cycle number, and the effect of cycle on the plateau pressures and plateau slopes were negligible. The effects of cycle test on the PCI behavior of the palladium-treated alloy powder samples were also tested, and the PCI behavior of the alloys' were the same as that of their corresponding inks. Those results show that the effect of ink preparation processes and the binders on the PCI of the alloys was small.

The amount of binder in the ink was low, i.e. 0.5–2 wt.% for both $LaNi_{4.7}Al_{0.3}$ and $CaNi_5$ alloys. The as-received ink surfaces were quite smooth, and the inks kept their structural integrities during the cycle test in un-humidified hydrogen for most of the test time. No loose powder or blisters were found on the thin-film inks after the tests. Before the cycle test, the particle size of $LaNi_{4.7}Al_{0.3}$ was less than 15 μm, and after 5000 cycles, the particle size was about 2 μm, i.e. the particle size decreased about 8 times. For $CaNi_5$ PEO ink, the particle size of $CaNi_5$ was about 50 μm before the test, and after 5000 cycles, the particle size was about 5 μm, i.e. a decrease of about 10 times.

Fig. 10 shows the absorption curve of palladium-treated $LaNi_{4.7}Al_{0.3}$ PVDF ink tested under 75% relative humidity hydrogen, the equilibrium H/M of the ink as a function of cycle number is shown in Fig. 11. With increasing the absorption/desorption cycle number, both the equilibrium H/M and initial hydrogen absorption rate decreased. The decreased rate of equilibrium H/M was linear with the cycle number. Unlike the test in the un-humidified

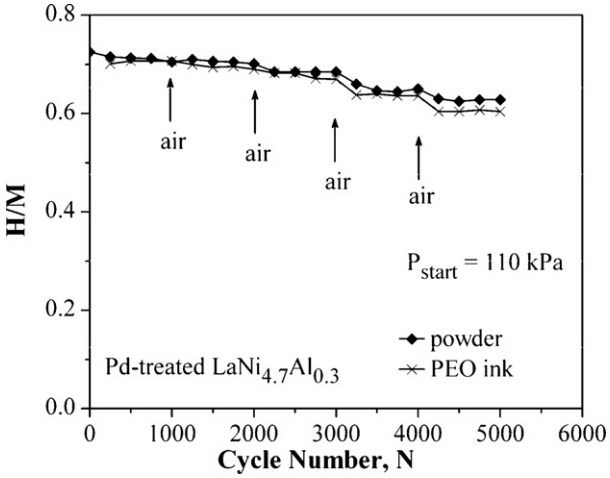

Fig. 7. Effect of absorption/desorption cycles on the absorption equilibrium H/M of Pd-treated $LaNi_{4.7}Al_{0.3}$ powder and PEO ink in un-humidified hydrogen.

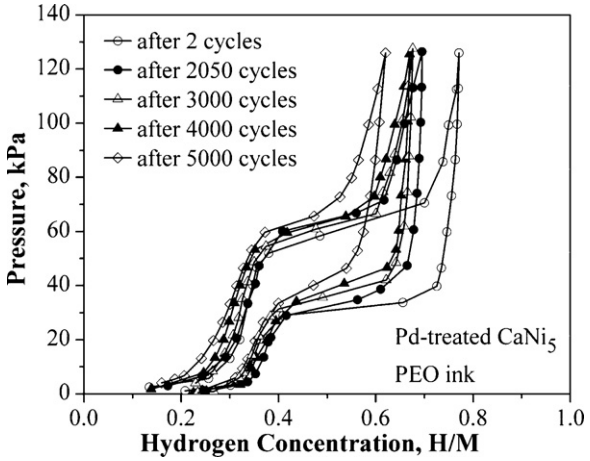

Fig. 9. Effect of absorption/desorption cycles on PCI of Pd-treated $CaNi_5$, PEO ink in un-humidified hydrogen.

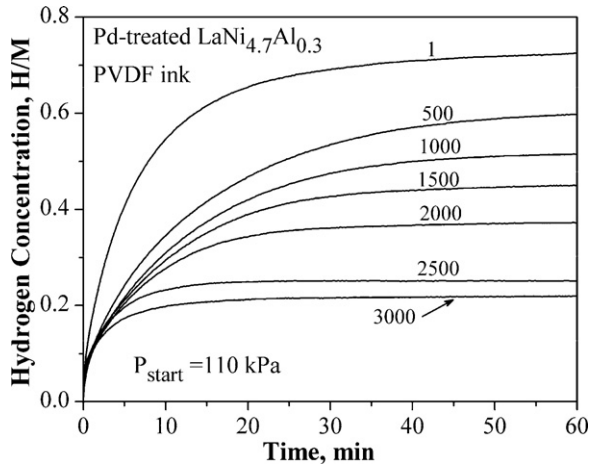

Fig. 10. Effect of absorption/desorption cycles on the absorption of Pd-treated $LaNi_{4.7}Al_{0.3}$ PVDF ink in hydrogen with 75% relative humidity.

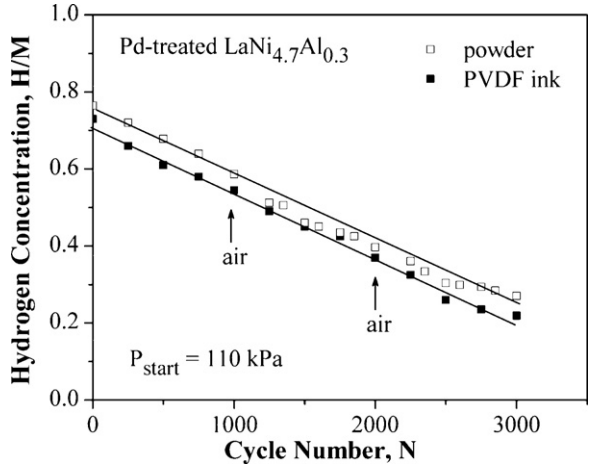

Fig. 11. Effect of absorption/desorption cycles on the absorption equilibrium H/M of Pd-treated $LaNi_{4.7}Al_{0.3}$ and PVDF ink in hydrogen with 75% relative humidity.

hydrogen, the air exposure after each one thousand cycles had no apparent effect on the equilibrium H/M in the following test period.

Water vapor in the hydrogen had significant effect on the PCI behaviors of the alloys in the cycle tests. Fig. 12 shows the PCI of the

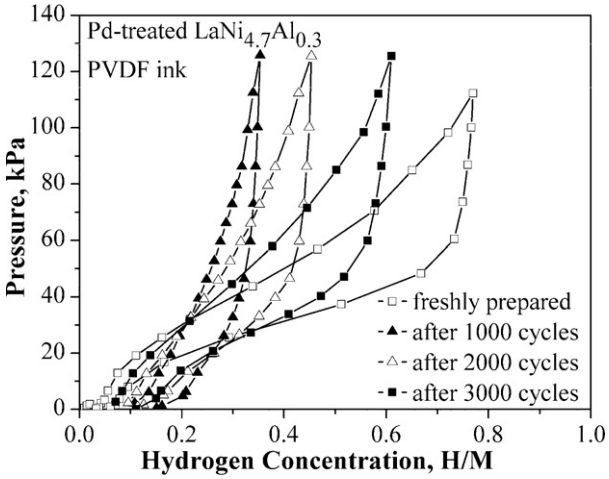

Fig. 12. Effect of absorption/desorption cycles on PCI of Pd-treated $LaNi_{4.7}Al_{0.3}$ PVDF ink in hydrogen with 75% relative humidity.

palladium-treated $LaNi_{4.7}Al_{0.3}$ PVDF ink before cycle test and after 1000, 2000 and 3000 hydrogen absorption/desorption cycles in 75% relative humidity hydrogen. With increasing cycle number, both the slopes of the absorption and desorption plateaus increase, and the widths of the plateau regions decreased, so the usable amount of absorbed hydrogen decreased. The PCI of the palladium-treated $LaNi_{4.7}Al_{0.3}$ powder sample as a function of cycle number under the same humidity hydrogen, and the same PCIs as the ink sample were obtained. By comparing the PCIs of the ink sample to the powder sample tested under the same condition, the polymer binder showed no effect on the cycle stability of $LaNi_{4.7}Al_{0.3}$ powder in humidity hydrogen.

In general, the overall ink structural integrity was not significantly affected by the cycle test with the presence of water vapor. Fig. 13 shows the morphology changes of palladium-treated $LaNi_{4.7}Al_{0.3}$ PVDF ink tested under 75% relative humidity hydrogen with increasing the hydrogen absorption/desorption cycle number. After the first 1000 cycles, one piece of ink with the size of several square mm peeled off from the ceramic slide at the corner of the ink. Other than that, the other part of the ink kept its overall structural integrity. Before the test, the surface of the ink was smooth and uniform, with increasing the cyclic number, the roughness of the ink surface increased. With increasing the absorption/desorption cycles, the particle size decreased dramatically, and after 3000 cycles, the particle size of $LaNi_{4.7}Al_{0.3}$ decreased from 15 to 20 μm to around 2 μm as shown in Fig. 13.

4. Discussion

The mechanism for increased performance and durability of the palladium-treated alloys was determined [13]. Degradation of performance for un-treated alloys is related to oxidation of the alloy surface and enhanced performance is related to beneficial effect of palladium. The beneficial effect of palladium in general for hydrogen reactivity is related to enhanced hydrogen spillover in the absorption process and reverse hydrogen spillover in the desorption process [16–20]. The deactivation of the hydrogen storage alloys is related to the oxidation of the alloy surfaces, which greatly reduces the hydrogen reactivity of the alloy's surface [21–24]. Palladium is stable and well known for its capacity to dissociate molecular hydrogen. When palladium particles are attached to the alloys' surfaces, molecular hydrogen can be dissociated into hydrogen atoms on palladium. The hydrogen atoms are spilt-over to the alloy surface, diffuse through the oxide layer and react with the alloy [13]. As long as palladium is in metallic state and attached to the intermetallic particle surface, hydrogen spillover and reverse hydrogen spillover can occur, and the alloys are active.

XPS analysis results indicate that after 5000 absorption/desorption cycles in un-humidified hydrogen, the binding energy of $Pd3d^{5/2}$ and $Pd3d^{3/2}$ are 335.1 and 330.5 eV respectively, which correspond to metallic palladium. No chemical changes were observed for palladium. Fukada [25] showed that palladium can keep its hydrogen absorption/desorption properties and has no microscopic changes for more than 1000 cycles. These results indicate that the catalytic effect of palladium should not be affected by the cycle tests. Therefore, degradation of palladium-treated $LaNi_{4.7}Al_{0.3}$ and $CaNi_5$ were not caused by the deactivation of palladium.

Intermetallic compounds are usually metastable phases and have the tendency to break up metallurgically to form stable, not easily reversed hydrides during the absorption/desorption cycle test, a process called disproportionation [26]. Fig. 14 shows the XRD results of the palladium-treated $LaNi_{4.7}Al_{0.3}$ PEO ink before test and after 1000, 3000 and 5000 cycles in un-humidified hydrogen. Except that the peak intensity ratio between palladium and

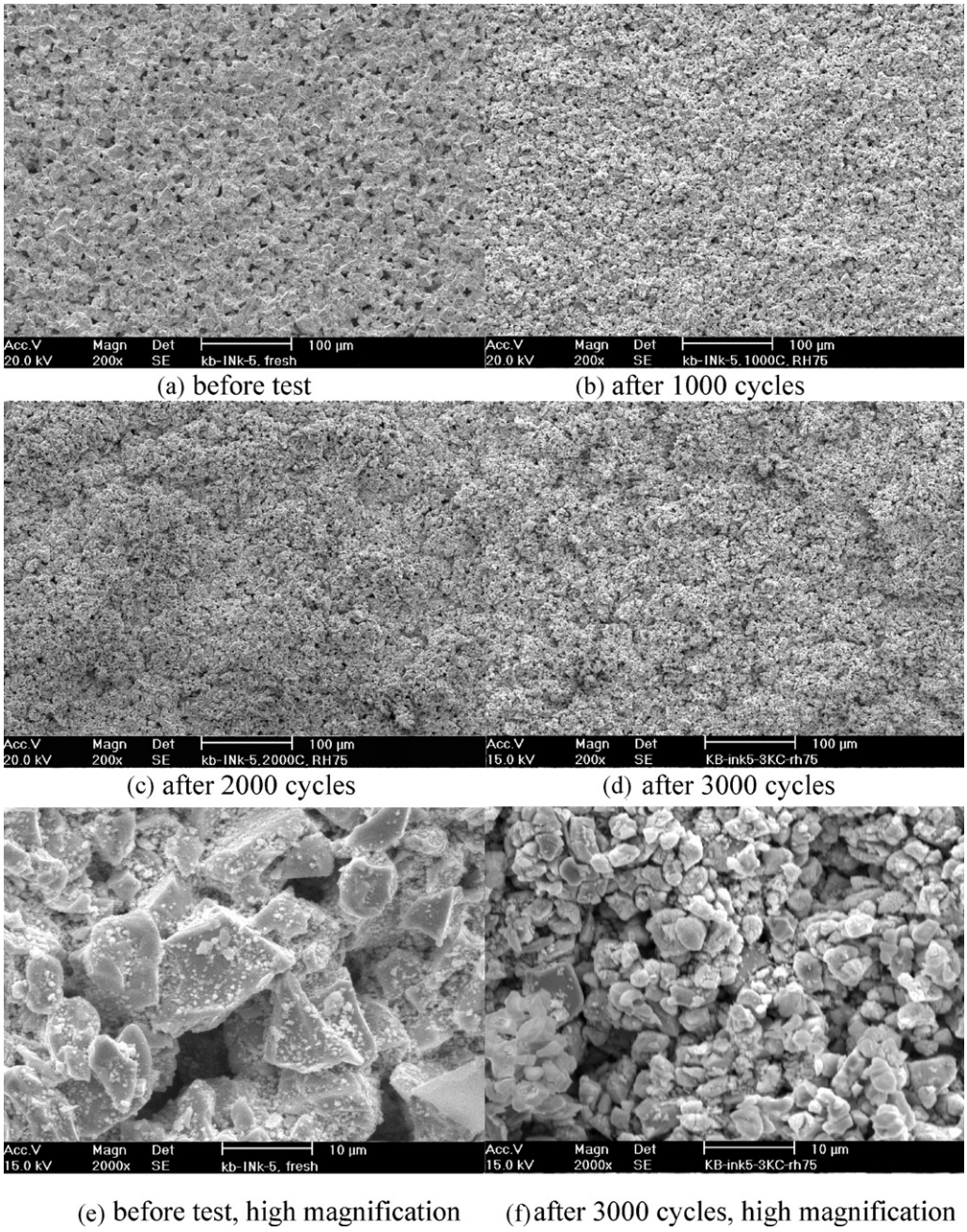

Fig. 13. Effect of absorption/desorption cycles on the morphology of Pd-treated $LaNi_{4.7}Al_{0.3}$ PVDF ink in hydrogen with 75% relative humidity: (a) before test, (b) after 1000 cycles, (c) after 2000 cycles, (d) after 3000 cycles, (e) before test, high magnification, (f) after 3000 cycles, high magnification.

$LaNi_{4.7}Al_{0.3}$ increases slightly. The diffraction pattern of $LaNi_{4.7}Al_{0.3}$ does not change with increasing cycle number. This is in agreement with Suzuki's result [27] which showed that after 2000 hydrogen absorption/desorption cycles, the X-ray diffraction pattern of $LaNi_{4.7}Al_{0.3}$ did not change. Therefore, the alloy's phase structure is unchanged during the cycle test, and the main reason for the capacity decrease of $LaNi_{4.7}Al_{0.3}$ is not due to disproportionation of the alloy.

The results showed that under un-humidified hydrogen, after 5000 cycles, the equilibrium H/M decreased 14–20% for the palladium-treated $LaNi_{4.7}Al_{0.3}$ powder and PEO ink samples, and the decrease mainly happened when the samples were exposed to air. Further, the air exposure after each 1000 cycles was the main reason for the capacity decrease of the palladium-treated $LaNi_{4.7}Al_{0.3}$ powder and ink. The air exposure leads to the oxidation of the particle surface. The surface area increases with increasing absorption/desorption cycles because of the decrepitation of the alloy particles. This leads to an increase in the amount of oxides formed during air exposure with increasing cycle number. The surface oxidation has two effects. One is the decrease of the amount of usable $LaNi_{4.7}Al_{0.3}$, and another is the deactivation of parts of the powder particles. As the SEM results show, with increasing absorption/desorption cycle number, alloy particles start to break into smaller particles due to decrepitation. Some of the smaller particles have no palladium particles attached to the surface, and they are also separated from other particles or far away from the particles that have palladium on the surfaces. During the air exposure, these particles were deactivated by the air exposure. In the absorption process, it is hard for hydrogen atoms formed on the palladium surface to diffuse to these particles, so these particles stop

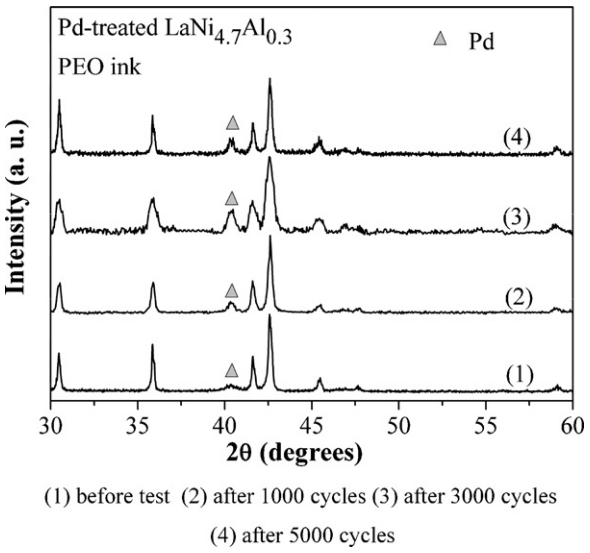

Fig. 14. XRD of Pd-treated $LaNi_{4.7}Al_{0.3}$ PEO ink after cycles in un-humidified hydrogen: (1) before test, (2) after 1000 cycles, (3) after 3000 cycles, (4) after 5000 cycles.

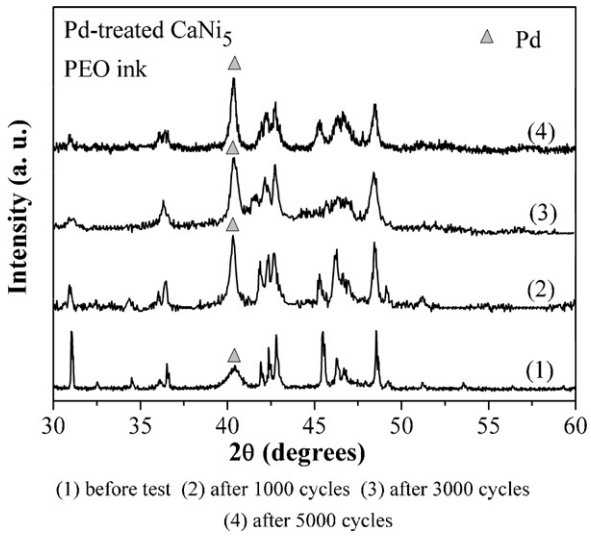

Fig. 16. XRD of Pd-treated $CaNi_5$ PEO ink after cycles in un-humidified hydrogen: (1) before test, (2) after 1000 cycles, (3) after 3000 cycles, (4) after 5000 cycles.

absorbing hydrogen under atmospheric pressure hydrogen at room temperature. The number of this type of isolated particles increases with increasing cycle numbers because of the decrease of the particle size. This leads to the decrease of the amount of hydrogen absorbed.

Exposure to the water vapor decreases the storage capacity of palladium-treated $LaNi_{4.7}Al_{0.3}$ during the cycle test under 75% relative humidity. Fig. 15 shows the XRD results of PVDF ink after tested under hydrogen with 75% relative humidity. The degradation mechanism for $LaNi_{4.7}Al_{0.3}$ tested under un-humidified hydrogen should also account for the degradation of $LaNi_{4.7}Al_{0.3}$ tested under humidified condition. It was reported that H_2O can split on the $LaNi_{4.7}Al_{0.3}$ or palladium surface, and this results in surface oxidation [28]. The water vapor reacts with the alloy and forms an amorphous phase on the surface [29]. Water vapor can also greatly reduce the reactivity of hydrogen dissociation on the $LaNi_{4.7}Al_{0.3}$ surface, and the effect of water vapor on the hydrogen reactivity is even stronger than that of oxygen [21,30]. During cycle tests in humidified hydrogen tests, the water vapor existed in the hydrogen all the time, as opposed to the tests in un-humidified hydrogen, in which exposure to humidity occurred only during integrity examination break. This continuous exposure to moisture made the attack of the water vapor much more severe.

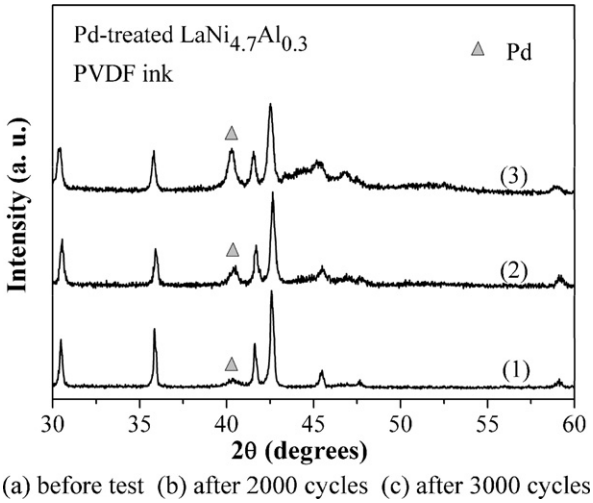

Fig. 15. XRD of Pd-treated $LaNi_{4.7}Al_{0.3}$ PVDF ink after cycles in hydrogen with 75% relative humidity: (a) before test, (b) after 2000 cycles, (c) after 3000 cycles.

For $CaNi_5$, though oxidation-induced degradation likely contributes to degraded performance, the degradation is mainly caused by disproportion. Fig. 16 shows the X-ray diffraction pattern of palladium-treated $CaNi_5$ PEO ink before the cycle test and after 1000, 3000 and 5000 absorption/desorption cycles in un-humidified hydrogen. With increasing cycle number, the X-ray diffraction pattern shows two effects. One effect is the increase of the $CaNi_5$ peaks width, and the other is the increase of the relative intensity of the palladium peak. By checking the count per second (CPS) of the diffraction peaks, it is found that the relative intensity change of palladium is mainly due to the decrease of the $CaNi_5$ diffraction peaks, and the CPSs of the palladium peaks remain almost unchanged with increasing cycle number. The XRD results of $CaNi_5$ show that the structure of $CaNi_5$ changed during the cycle test, while palladium remained unchanged. The $CaNi_5$ is not a stable phase and disproportionation tends to occur during absorption/desorption process [31]. The disproportionation products, such as Ni, form oxide on the surface during the air exposure, and this leads the relative intensity decrease of the XRD diffraction peaks of $CaNi_5$.

5. Conclusion

(1) The palladium-treated intermetallic hydrogen storage alloys are compatible with a thin-film micro-fabrication process. During the fabrication, the alloys are exposed to air, polymer binders and solvents. The inks made with palladium-treated alloys have good air exposure durability, while un-treated powders are inactive or lose activity. The thin-film inks made with the palladium-treated alloys can absorb hydrogen readily at atmospheric pressure. The absorption/desorption rates remain fast even after the ink was exposed to air for more than 47 weeks.

(2) The effect of the absorption/desorption cycles on the absorption rates of the palladium-treated alloys is small in pure hydrogen. Even after being exposed to air for up to 72 h during the cycle test, the palladium-treated alloys can still absorb hydrogen readily under atmospheric hydrogen and maintain fast hydrogen absorption rate.

(3) The effect of the absorption/desorption cycles on the hydrogen storage capacity of the palladium-treated alloys varies with the alloys tested in pure hydrogen. The $LaNi_{4.7}Al_{0.3}$ has better stability than $CaNi_5$. For $LaNi_{4.7}Al_{0.3}$, the air exposure during intermittent sample examination in the cycle test caused the oxidation of small amount of isolated particles formed by decrepitation, and this prevents hydrogen atoms formed on the palladium from diffusing to these particles. This led to a minor decrease of storage capacity of $LaNi_{4.7}Al_{0.3}$ after the air exposure during the absorption/desorption cyclic test. The capacity decrease of $CaNi_5$ during the absorption/desorption cycle test was greater than $LaNi_{4.7}Al_{0.3}$ and was mainly due to the disproportionation of $CaNi_5$.

(4) The palladium-treated alloys and inks made with these alloys can keep the sub-atmosphere hydrogen absorption performance with the existence of high amount of water vapor in the hydrogen gas, although the amount of water vapor in the hydrogen gas increased the degradation of palladium-treated $LaNi_{4.7}Al_{0.3}$. The main reason for the more degradation is the oxidation of $LaNi_{4.7}Al_{0.3}$, which is accelerated by the existence of water in the hydrogen gas.

(5) The inks maintained overall structural integrity during the hydrogen absorption/desorption cyclic tests. There was little or no loss of adhesion of alloy particles.

Acknowledgements

This work was supported in part by the National Institutes of Health NINDS Grant No. NS-041809 and NIBIB Grant No. EB-001740. Joe H. Payer and Xi Shan acknowledge the collaboration and support of their colleagues at Case Western Reserve University.

References

[1] J.S. Wainright, R.F. Savinell, C.C. Liu, M. Litt, Electrochim. Acta 48 (2003) 2869.
[2] W.G. Tam, J.S. Wainright, J. Power Sources 165 (2007) 481.
[3] W.G. Tam, J.S. Wainright, ECS Trans. 1 (2006) 1.
[4] T.B. Flanagan, W.A. Oates, Annu. Rev. Mater. Sci. 21 (1991) 269.
[5] F.A. Lewis, The Palladium Hydrogen System, Academic press, 1967.
[6] X.L. Wang, S. Suda, Zeitschrift fur Physikalische Chemie 183 (1994) 385.
[7] X.L. Wang, S. Suda, J. Alloys Compd. 194 (1993) 73.
[8] D.B. Willey, D. Pederzolli, A.S. Pratt, J. Swift, A. Walton, I.R. Harris, J. Alloys Compd. 330–332 (2002) 806.
[9] L. Zaluski, A. Zaluska, J.O. Strom-Olsen, J. Alloys Compd. 253–254 (1997) 70.
[10] W. Oelerich, T. Klassen, R. Bormann, J. Alloys Compd. 322 (2001) L5.
[11] L. Zaluski, A. Zaluska, P. Tessier, J. Mater. Sci. 31 (1996) 695.
[12] X. Shan, J.H. Payer, J. Wainright, J. Alloys Compd. 426 (2006) 400.
[13] X. Shan, J.H. Payer, W.D. Jennings, Int. J. Hydrogen Energy 34 (2009) 363.
[14] X. Shan, J.H. Payer, J. Wainright, J. Alloys Compd. 430 (2007) 262.
[15] International Organization of Legal Metrology, publication no.: OIML R 121, The scale of relative humidity of air certified against saturated salt solutions, 1996 ed.
[16] W.C. Conner, in: D.D. Eley, H. Pines (Eds.), Advances in Catalysis, vol. 34, Academic Press, Inc., Orlando, 1986, pp. 1–79.
[17] P.A. Sermon, G.C. Bond, in: H. Heinemann (Ed.), Catalysis Reviews, vol. 8, Marcel Dekker, Inc., New York, 1973, pp. 211–239.
[18] W.C. Conner, J.L. Falconer, Chem. Rev. 95 (1995) 759.
[19] W.C. Conner, J.F. Cevallos-Candau, in: G.M. Pajonk (Ed.), Spillover of Adsorbed Species, Elsevier Science, Netherlands, 1983.
[20] J. Nicole, J. Catal. 204 (2001) 23.
[21] H. Uchida, Zeitschrift Fur Physikalische Chemie 181 (1993), S.417.
[22] H. Uchida, M. Ozawa, Zeitschrift Fur Physikalische Chemie Neue Folge 147 (1986) 77.
[23] H. Uchida, J. Less Common Met. 172–174 (1991) 983.
[24] H. Uchida, Int. J. Hydrogen Energy 24 (1999) 861.
[25] S. Fukada, M. Samsun-Baharin, Int. J. Hydrogen Energy 27 (2002) 177.
[26] G. Sandrock, J. Alloys Compd. 293 (1999) 877.
[27] K. Suzuki, K. Ishikawa, K. Aoki, Mater. Trans. JIM 41 (2000) 581.
[28] G.D. Sandrock, J. Less Common Met. 73 (1980) 161.
[29] S Yamakawa, J. Jpn. Inst. Met. 67 (2003) 53.
[30] H. Uchida, Zeitschrift Fur Physikalische Chemie 183 (1994), S.303.
[31] G.D. Sandrock, Mater. Res. Bull. 17 (1982) 887.